Spin-spin coupling at small x: Worm-gear and pretzelosity TMDs

M. Gabriel Santiago[*]

Center for Nuclear Femtography, SURA, 1201 New York Avenue NW, Washington, DC 20005 USA

We study the small-x asymptotics of the leading-twist quark transverse momentum dependent parton distribution functions (TMDs) which encode couplings between the polarization of the quarks and that of their parent hadron, with at least one of the two polarizations in the transverse direction: the two worm-gear TMDs g_{1T} and $h_{1L}^\perp$, and the pretzelosity $h_{1T}^\perp$. We apply the light cone operator treatment which has been developed in recent years to rewrite the TMD operator definitions at small-x in terms of polarized dipole amplitudes, finding that in the flavor nonsinglet sector all three TMDs reduce in the small-x limit to previously known polarized dipole amplitudes, and thus the large-N_c, linearized, double logarithmic approximation (DLA) asymptotics have all been solved for previously. We have compiled these asymptotics together with those of the other five flavor nonsinglet, leading-twist quark TMDs into a single unified table.

I. INTRODUCTION

The intersection of quantum chromodynamics (QCD) at small Bjorken x and spin physics has been the topic of a surge of recent research activity [1–48]. In particular, the inclusion of subeikonal and sub-subeikonal corrections [6,9,12,16–20,23–27,30–33,36–40,43,48] to the saturation/ Color Glass Condensate (CGC) framework [49–57] has been explored in detail, both in the study of transverse momentum dependent parton distribution functions (TMDs) at small-x as well as in the direct study of quark and gluon propagators through the strong gluon field background of the CGC. This extension of the saturation framework allows one to go beyond the Collins-Soper-Sterman evolution equations [58–62] which resum logarithms of the hard scale Q^2, and instead resum logarithms of $1/x$ to predict the small-x behavior of TMDs. Using the light cone operator treatment (LCOT) originally developed in [9,20,23,24,36], the evolution of several leading-twist quark and gluon TMDs has been studied by constructing polarized dipole amplitudes containing spin-dependent subeikonal and sub-subeikonal corrections to the usual eikonal, small-x dipole amplitudes. Including the unpolarized quark TMD, which has small-x behavior determined by the evolution equation for the Reggeon [63–68], five of the eight leading-twist quark TMDs have known small-x asymptotics. In this work, we

will study the small-x asymptotics of the remaining three leading-twist quark TMDs, the two worm-gear TMDs, g_{1T} and $h_{1L}^\perp$, and the pretzelosity $h_{1T}^\perp$. These three TMDs vanish upon integration over the quark transverse momentum k_T, and encode various couplings between the polarization of the quarks with the polarization of their parent hadron [69]. Studying their small-x asymptotics will give us a window into this spin-spin coupling structure in the gluon dominated, high energy regime of QCD. We will apply the LCOT to all three TMD operator definitions, then find the asymptotics of the flavor nonsinglet TMDs in the large-N_c limit, further taking the linearized double logarithmic approximation (DLA).

The structure of the remainder of this paper is as follows: we will start in Sec. II with the worm-gear g_{1T} function, finding that in the small-x limit it reduces to the same polarized dipole amplitudes which are present in the sub-eikonal contribution to the Sivers function [44], but with a crucial change from the real part of a correlator to the imaginary part. This alters the initial conditions for the evolution of the polarized dipole amplitudes, and leads to the same evolution equations as for the sub-subeikonal Boer-Mulders function [44], yielding x-independent, exactly subeikonal asymptotics

$$g_{1T}^{\mathrm{NS}}(x \ll 1, k_T^2) \sim \left(\frac{1}{x}\right)^0. \tag{1}$$

Next in Sec. III we will study the worm-gear $h_{1L}^\perp$ function. It will turn out to share analogous polarized dipole amplitudes to the sub-subeikonal Boer-Mulders function [44], leading to exactly sub-subeikonal scaling

[*]gsantiago@sura.org

TABLE I. The collected leading small-x asymptotics for the leading-twist flavor nonsinglet quark TMDs. The intercept of the unpolarized quark TMD f_1 was found from the evolution equation for the Reggeon [63–68] and also with the infrared evolution equation (IREE) [70], while the remaining seven intercepts have been calculated using the LCOT in [9,20,23,24,44] and this work. The intercept for the flavor nonsinglet helicity TMD was also found in [71] using the IREE and agrees with the result found using the LCOT. Finally, the intercept of the flavor nonsinglet transversity TMD found in the LCOT matches that found in [72].

		Leading twist quark TMDs		
		Quark polarization		
		U	L	T
Nucleon polarization	U	$f_1^{\mathrm{NS}} \sim x^{-\sqrt{2\alpha_s C_F/\pi}}$		$h_1^{\perp\mathrm{NS}} \sim x$
	L		$g_1^{\mathrm{NS}} \sim x^{-\sqrt{\alpha_s N_c/\pi}}$	$h_{1L}^{\perp\mathrm{NS}} \sim x$
	T	$f_{1T}^{\perp\mathrm{NS}} \sim C_{\mathcal{O}}x^{-1} + C_1 x^{-3.4\sqrt{\alpha_s N_c/4\pi}}$	$g_{1T}^{\mathrm{NS}} \sim x^0$	$h_1^{\mathrm{NS}} \sim h_{1T}^{\perp\mathrm{NS}} \sim x^{1-2\sqrt{\alpha_s N_c/2\pi}}$

$$h_{1L}^{\perp\mathrm{NS}}(x \ll 1, k_T^2) \sim \left(\frac{1}{x}\right)^{-1}, \qquad (2)$$

giving with g_{1T} two examples of time reversal even (T-even) TMDs which receive essentially no corrections to their naive scaling with x in the linearized evolution regime. We continue on to Sec. IV where we study the pretzelosity TMD, finding that it shares polarized dipole amplitudes with the transversity TMD [23] and has the same asymptotic scaling as

$$h_{1T}^{\perp\mathrm{NS}}(x \ll 1, k_T^2) \sim \left(\frac{1}{x}\right)^{-1+2\sqrt{\frac{\alpha_s N_c}{2\pi}}}, \qquad (3)$$

coming from the evolution equation for the Reggeon [63–68]. Finally, in Sec. V we summarize our results and point out some directions for future work. We have collected these asymptotics together with those for the other leading-twist quark TMDs in Table I.

Throughout this paper we will make use of light-cone coordinates $u = (u^+ = u^0 + u^3, u^- = u^0 - u^3, \underline{u})$, labeling the transverse part of a four-vector u as $\underline{u}$ except in the case of an integral measure, where it will be denoted as $u_\perp$, and in the case of the quark transverse momentum argument of a TMD, where we will use the conventional label k_T. We will also make use of Brodsky-Lepage (BL) spinors [73], specifically in the plus-minus reversed form defined as [23,24]

$$u_\sigma(p) = \frac{1}{\sqrt{p^=}}[p^- + m\gamma^0 + \gamma^0\underline{\gamma}\cdot\underline{p}]\rho(\sigma),$$

$$v_\sigma(p) = \frac{1}{\sqrt{p^=}}[p^- - m\gamma^0 + \gamma^0\underline{\gamma}\cdot\underline{p}]\rho(-\sigma), \qquad (4)$$

with $p^\mu = (\frac{p^2+m^2}{p^-}, p^-, \underline{p})$ and

$$\rho(+1) = \frac{1}{\sqrt{2}}\begin{pmatrix} 1 \\ 0 \\ -1 \\ 0 \end{pmatrix}, \qquad \rho(-1) = \frac{1}{\sqrt{2}}\begin{pmatrix} 0 \\ 1 \\ 0 \\ 1 \end{pmatrix}. \qquad (5)$$

We will refer to these as anti BL spinors.

II. WORM-GEAR g_{1T}

We begin with the worm-gear TMD g_{1T}, which can be interpreted as the number density of longitudinally polarized quarks within a transversely polarized proton. It is defined as [74]

$$\frac{k_T \cdot S_P}{M_P} g_{1T}(x, k_T^2) = \int \frac{\mathrm{d}r^- \, \mathrm{d}^2 r_\perp}{2(2\pi)^3} \langle P, S_P|\bar{\psi}(0)\mathcal{U}[0, r]$$
$$\times \frac{\gamma^+\gamma_5}{2}\psi(r)|P, S_P\rangle, \qquad (6)$$

where the proton spin S_P is in the transverse plane and we take the future pointing semi-inclusive deep inelastic scattering (SIDIS) staple gauge link $U[0, r] = V_0[0, \infty]V_r[\infty, r^-]$ with fundamental light-cone Wilson lines defined as

$$V_{\underline{x}}[x_f^-, x_i^-] = \mathcal{P}\exp\left[\frac{ig}{2}\int_{x_i^-}^{x_f^-} \mathrm{d}x^- A^+(0^+, x^-, \underline{x})\right]. \qquad (7)$$

We have dropped the transverse pieces of the gauge link out at infinity, so we must work in a nonsingular gauge. Here we will take the proton "target" to be moving along the x^+ direction, and will work in $A^- = 0$ gauge for our calculations. We apply the LCOT [23,24], rewriting the matrix element as a small-x quasi-classical average in the target proton state [27,75–80]

$$\frac{k_T \cdot S_P}{M_P} g_{1T}(x, k_T^2) \subset \frac{2p_1^+}{2(2\pi)^3} \sum_X \int d\xi^- d^2\xi_\perp d\zeta^- d^2\zeta_\perp e^{ik\cdot(\xi-\zeta)}$$

$$\times \left[\frac{\gamma^+\gamma_5}{2}\right]_{\alpha\beta} \langle\bar\psi_\alpha(\xi) V_{\underline\xi}[\xi^-, \infty]|X\rangle$$

$$\times \langle X|V_{\underline\zeta}[\infty, \zeta^-]\psi_\beta(\zeta)\rangle. \tag{8}$$

Here we have inserted a sum over the complete set of states $|X\rangle$, and the outer angular brackets indicate the quasi-classical averaging over the proton wave function.

One can show that the eikonal contribution to this TMD vanishes, just as for the other quark spin dependent leading-twist quark TMDs. The leading contribution then comes from diagrams of the class shown in Fig. 1, where we have taken $|X\rangle$ to be an antiquark state and added a subeikonal spin-dependent exchange (the white box) onto the Wilson line which encodes the interactions between the antiquark and the target as it passes through the shock wave [the blue (gray) rectangle]. Evaluating these diagrams (cf. [23,24]) yields the subeikonal contribution to the worm-gear function as

$$\frac{k_T \cdot S_P}{M_P} g_{1T}(x, k_T^2)|_{\text{subeik}}$$

$$\subset \frac{-2p_1^+}{2(2\pi)^3} \int d^2\zeta_\perp d^2w_\perp d^2z_\perp \frac{dk_1^- d^2k_{1\perp}}{(2\pi)^3}$$

$$\times \frac{e^{i\underline{k}_1\cdot(\underline{w}-\underline\zeta)+i\underline{k}\cdot(\underline{z}-\underline\zeta)}\theta(k_1^-)}{(xp_1^+ k_1^- + \underline{k}_1^2)(xp_1^+ k_1^- + \underline{k}^2)}$$

$$\times \sum_{\sigma_1,\sigma_2}\bar v_{\sigma_2}(k_2)\frac{\gamma^+\gamma_5}{2} v_{\sigma_1}(k_1)\langle \text{T}V_{\underline\zeta}^{ij}\bar v_{\sigma_1}(k_1)\hat V_{\underline{z},\underline{w}}^{\dagger ji}$$

$$\times v_{\sigma_2}(k_2)\rangle\Big|_{k_1^-=k_2^-,\underline{k}_1^2=\underline{k}_2^2=0,\underline{k}_2=-\underline{k}} + \text{c.c.} \tag{9}$$

We now need the anti BL spinor product

$$\bar v_{\sigma_2}(k_2)\frac{\gamma^+\gamma_5}{2} v_{\sigma_1}(k_1) = \frac{1}{2}\frac{\sigma_2\delta_{\sigma_2,\sigma_1}(\underline{k}_2\cdot\underline{k}_1) - i\delta_{\sigma_2,\sigma_1}(\underline{k}_2\times\underline{k}_1)}{\sqrt{k_2^- k_1^-}}, \tag{10}$$
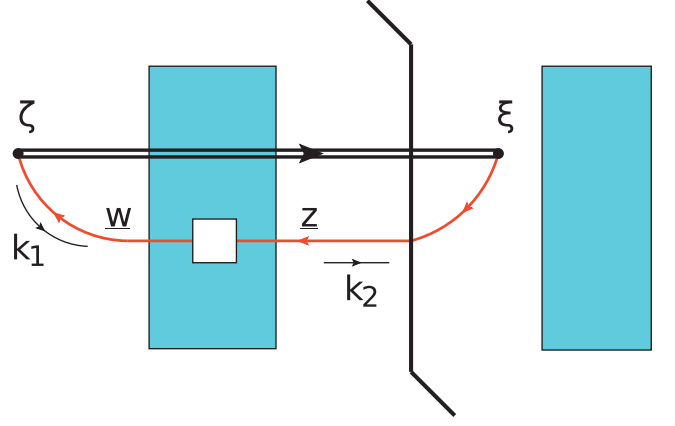
FIG. 1. Example of the class of diagrams which give the leading subeikonal and sub-subeikonal corrections for the TMDs considered here. The antiquark propagates from the position ζ to $\underline{w}$ with momentum k_1, undergoes a subeikonal interaction with the proton which changes its transverse position from $\underline{w}$ on the left of the shock wave to $\underline{z}$ on the right of the shock wave. The antiquark then propagates from $\underline{z}$ to the position ξ with momentum k_2. The shock wave is denoted by the blue (gray) rectangle, while the sub-(sub) eikonal interaction with the shock wave is denoted by the white box. The double line represents the eikonal Wilson line encoding the interactions of the quark in the dipole.

as well as the replacement [43,44]

$$\int d^2z_\perp \bar v_{\sigma_1}(k_1)\big(\hat V_{\underline{z},\underline{w}}^\dagger\big)^{ji} v_{\sigma_2}(k_2)$$

$$\to 2\sqrt{k_1^- k_2^-}\int d^2z_\perp \big(V_{\underline{z},\underline{w};\sigma_2,\sigma_1}^{\text{pol}\dagger}\big)^{ji}, \tag{11}$$

where we have the polarized Wilson line

$$V_{\underline{x},\underline{y};\sigma',\sigma}^{\text{pol}} = \delta_{\sigma,\sigma'} V_{\underline{x},\underline{y}}^{\text{phase}} - \sigma\delta_{\sigma,\sigma'} V_{\underline{x},\underline{y}}^{\text{mag}} \tag{12}$$

with

$$V_{\underline{x},\underline{y}}^{\text{phase}} = -\frac{ip_1^+}{2s}\int_{-\infty}^\infty dz^- d^2z_\perp V_{\underline{x}}[\infty, z^-]\delta^2(\underline{x}-\underline{z})\bar D_{\underline{z}}^i \bar D_{\underline{z}}^i V_{\underline{y}}[z^-, -\infty]\delta^2(\underline{y}-\underline{z})$$

$$-\frac{g^2 p_1^+}{4s}\delta^2(\underline{x}-\underline{y})\int_{-\infty}^\infty dz_1^-\int_{z_1^-}^\infty dz_2^- V_{\underline{x}}[\infty, z_2^-]t^b\psi_\beta(z_2^-, \underline{x})U_{\underline{x}}^{ba}[z_2^-, z_1^-]\left[\frac{\gamma^+}{2}\right]_{\alpha\beta}\bar\psi_\alpha(z_1^-, \underline{x})t^a V_{\underline{x}}[z_1^-, -\infty], \tag{13a}$$

$$V_{\underline{x},\underline{y}}^{\text{mag}} = \frac{igp_1^+}{2s}\delta^2(\underline{x}-\underline{y})\int_{-\infty}^\infty dz^- V_{\underline{x}}[\infty, z^-]F^{12}V_{\underline{x}}[z^-, -\infty]$$

$$-\frac{g^2 p_1^+}{4s}\delta^2(\underline{x}-\underline{y})\int_{-\infty}^\infty dz_1^-\int_{z_1^-}^\infty dz_2^- V_{\underline{x}}[\infty, z_2^-]t^b\psi_\beta(z_2^-, \underline{x})U_{\underline{x}}^{ba}[z_2^-, z_1^-]\left[\frac{\gamma^+\gamma^5}{2}\right]_{\alpha\beta}\bar\psi_\alpha(z_1^-, \underline{x})t^a V_{\underline{x}}[z_1^-, -\infty]. \tag{13b}$$

neglecting terms proportional to the quark masses. Here ψ and $\bar{\psi}$ are the background quark and antiquark fields of the target hadron, F^{12} is a component of the background gluon field strength tensor, and $\vec{D}^i = \vec{\partial}_i - igA^i$, $\bar{D}^i = \bar{\partial}_i + igA^i$ are the left and right acting fundamental representation covariant derivatives. We have also introduced the adjoint representation Wilson line

$$U_{\underline{x}}[x_f^-, x_i^-] = \mathcal{P} \exp\left[\frac{ig}{2}\int_{x_i^-}^{x_f^-} dx^- \mathcal{A}^+(0^+, x^-, \underline{x})\right] \tag{14}$$

with $U_{\underline{x}} \equiv U_{\underline{x}}[\infty, -\infty]$. Plugging Eqs. (10) and (11) into Eq. (9) yields

$$\begin{aligned}
\frac{k_T \cdot S_P}{M_P} g_{1T}(x, k_T^2)|_{\text{subeik}} &\subset \frac{2p_1^+}{(2\pi)^3} \int d^2\zeta_\perp d^2 w_\perp d^2 z_\perp \frac{dk_1^- d^2 k_{1\perp}}{(2\pi)^3} \theta(k_1^-) \frac{1}{(xp_1^+ k_1^- + \underline{k}_1^2)(xp_1^+ k_1^- + \underline{k}^2)} \\
&\times \left\langle i\underline{k}_1 \times \underline{k}\left(e^{i\underline{k}_1 \cdot (\underline{w}-\underline{\zeta}) + i\underline{k}\cdot(\underline{z}-\underline{\zeta})} \mathrm{Ttr}[V_{\underline{\zeta}} V_{\underline{z},\underline{w}}^{\text{phase}\dagger}] - e^{-i\underline{k}_1 \cdot(\underline{w}-\underline{\zeta})-i\underline{k}\cdot(\underline{z}-\underline{\zeta})} \bar{\mathrm{T}}\,\mathrm{tr}[V_{\underline{z},\underline{w}}^{\text{phase}} V_{\underline{\zeta}}^\dagger]\right) \\
&+ e^{i(\underline{k}_1+\underline{k})\cdot(\underline{w}-\underline{\zeta})} \underline{k}_1 \cdot \underline{k}\left(\mathrm{T}\,\mathrm{tr}[V_{\underline{\zeta}} V_{\underline{z},\underline{w}}^{\text{mag}\dagger}] + \bar{\mathrm{T}}\,\mathrm{tr}[V_{\underline{z},\underline{\zeta}}^{\text{mag}} V_{\underline{w}}^\dagger]\right)\right\rangle, \tag{15}
\end{aligned}$$

where we have interchanged $\underline{w}$ and $\underline{\zeta}$ in the last trace. We can recognize in Eq. (15) the exact same Wilson line correlators which are present in the subeikonal contribution to the Sivers function [44]. There the left-hand side (lhs) contained a cross product $k_T \times S_P$ and the right-hand side (rhs) had $\underline{k}_1 \cdot \underline{k}$ multiplying the $V_{\underline{z},\underline{w}}^{\text{phase}\dagger}$ correlator and $i\underline{k}_1 \times \underline{k}$ multiplying the $V_{\underline{z},\underline{w}}^{\text{mag}\dagger}$ correlator. The equation above changes the lhs cross product in the Sivers case to a dot product $k_T \cdot S_P$ here, and exchanges the $\underline{k}_1, \underline{k}$ structures on the rhs. Thus, as in the case of the Sivers function, the polarized dipole amplitude containing $V_{\underline{z},\underline{w}}^{\text{phase}\dagger}$ must bring in a factor of ϵ^{ij} and be linear in S_P once integrated over impact parameter, while the polarized dipole amplitude containing $V_{\underline{z},\underline{w}}^{\text{mag}\dagger}$ must have no factor of ϵ^{ij} and be linear in S_P once integrated over impact parameter. Having the same tensor structures in front of the impact parameter integrated polarized dipole amplitudes allows us to apply the results for the subeikonal contribution to the Sivers function to g_{1T}, taking the flavor non-singlet TMD, defined as the difference between the quark and antiquark TMDs

$$g_{1T}^{\text{NS}} = g_{1T}^q - g_{1T}^{\bar{q}}, \tag{16}$$

to obtain

$$\begin{aligned}
\frac{k_T \cdot S_P}{M_P} g_{1T}^{\text{NS}}(x, k_T^2)|_{\text{subeik}} &= \frac{8N_c p_1^+}{(2\pi)^3} \int d^2\zeta_\perp d^2 w_\perp \frac{d^2 k_{1\perp}}{(2\pi)^3} e^{i(\underline{k}+\underline{k}_1)\cdot(\underline{w}-\underline{\zeta})} \frac{1}{\underline{k}_1^2 \underline{k}^2} \\
&\times \int_{\Lambda/s}^1 \frac{dz}{z}\left[i\underline{k}_1 \times \underline{k}(\underline{k}-\underline{k}_1)^i G_{\underline{w}\underline{\zeta}}^i + i\underline{k}_1 \times \underline{k} G_{\underline{w}\underline{\zeta}}^{[2]}\right. \\
&\left.+ \underline{k}_1 \cdot \underline{k} G_{\underline{w}\underline{\zeta}}^{\text{mag}}\right], \tag{17}
\end{aligned}$$

with

$$G_{\underline{w}\underline{\zeta}}^i = \frac{1}{2N_c} \mathrm{Im}\left\langle\!\left\langle \mathrm{Ttr}[V_{\underline{\zeta}} V_{\underline{w}}^{i\dagger}] - \mathrm{Ttr}[V_{\underline{w}}^i V_{\underline{\zeta}}^\dagger]\right\rangle\!\right\rangle_1, \tag{18a}$$

$$G_{\underline{w}\underline{\zeta}}^{[2]} = \frac{1}{2N_c} \mathrm{Re}\left\langle\!\left\langle \mathrm{Ttr}[V_{\underline{\zeta}} V_{\underline{w}}^{[2]\dagger}] - \mathrm{Ttr}[V_{\underline{w}}^{[2]} V_{\underline{\zeta}}^\dagger]\right\rangle\!\right\rangle_1, \tag{18b}$$

$$G_{\underline{w}\underline{\zeta}}^{\text{mag}} = \frac{1}{2N_c} \mathrm{Im}\left\langle\!\left\langle \mathrm{Ttr}[V_{\underline{\zeta}} V_{\underline{w}}^{\text{mag}\dagger}] - \mathrm{Ttr}[V_{\underline{w}}^{\text{mag}} V_{\underline{\zeta}}^\dagger]\right\rangle\!\right\rangle_1 \tag{18c}$$

where the double angle brackets scale out powers of energy, $\langle\!\langle\ldots\rangle\!\rangle_n = (zs)^n \langle\ldots\rangle$. Here we have introduced the polarized Wilson lines

$$V_{\underline{x}}^i = \frac{p_1^+}{4s} \int_{-\infty}^\infty dz^- V_{\underline{x}}[\infty, z^-][\vec{D}_x^i - \bar{D}_x^i] V_{\underline{x}}[z^-, -\infty], \tag{19a}$$

$$\begin{aligned}
V_{\underline{x};\underline{k},\underline{k}_1}^{[2]} &= \frac{ip_1^+}{8s} \int_{-\infty}^\infty dz^- V_{\underline{x}}[\infty, z^-] \\
&\times [(\vec{D}_x^i - \bar{D}_x^i)^2 - (k_1^i - k^i)^2] V_{\underline{x}}[z^-, -\infty] \\
&- \frac{g^2 p_1^+}{4s} \int_{-\infty}^\infty dz_1^- \int_{z_1^-}^\infty dz_2^- V_{\underline{x}}[\infty, z_2^-] t^b \psi_\beta(z_2^-, \underline{x}) \\
&\times U_{\underline{x}}^{ba}[z_2^-, z_1^-]\left[\frac{\gamma^+}{2}\right]_{\alpha\beta} \bar{\psi}_\alpha(z_1^-, \underline{x}) t^a V_{\underline{x}}[z_1^-, -\infty] \tag{19b}
\end{aligned}$$

which were contained in Eq. (13).

The only difference between the dipole amplitudes in Eq. (18) and those in the subeikonal contribution to the flavor nonsinglet Sivers function [44] is the "Im" operator acting on the correlators containing $V_{\underline{x}}^i$ and $V_{\underline{x}}^{\text{mag}}$ in Eqs. (18a) and (18c), rather than a "Re" operator as in

the Sivers case, and vice versa for the correlator containing $V_{\underline{x}}^{[2]}$ in Eq. (18b). This change does not affect any of the evolution calculations at the level of the polarized Wilson line correlators, but it significantly changes the initial conditions for the polarized dipole amplitudes. We will argue below that the only polarized dipole amplitude which contributes to the linearized, DLA small-x asymptotics of the worm-gear g_{1T} is $G_{\underline{w}\underline{\zeta}}^{[2]}$, with all other amplitudes dropping out due to having initial conditions equal to zero and having no mixing with $G_{\underline{w}\underline{\zeta}}^{[2]}$ under evolution. This means we can simplify the worm-gear TMD further as

$$
\frac{k_T \cdot S_P}{M_P} g_{1T}^{\text{NS}}(x, k_T^2)\big|_{\text{subeik}}
$$

$$
= \frac{8 N_c p_1^+}{(2\pi)^3} \int d^2\zeta_\perp d^2 w_\perp \frac{d^2 k_{1\perp}}{(2\pi)^3} e^{i(\underline{k}+\underline{k}_1)\cdot(\underline{w}-\underline{\zeta})}
$$

$$
\times \frac{i\underline{k}_1 \times \underline{k}}{\underline{k}_1^2 \underline{k}^2} \int_{\Lambda/s}^1 \frac{dz}{z} G_{\underline{w}\underline{\zeta}}^{[2]}
$$

$$
= \frac{8 N_c p_1^+}{(2\pi)^3} \int d^2 x_{10} \frac{d^2 k_{1\perp}}{(2\pi)^3} e^{i(\underline{k}+\underline{k}_1)\cdot \underline{x}_{10}} \frac{i\underline{k}_1 \times \underline{k}}{\underline{k}_1^2 \underline{k}^2}
$$

$$
\times \int_{\Lambda/s}^1 \frac{dz}{z}(\underline{x}_{10} \times \underline{S}_P) G^{[2]}(x_{10}^2, z), \tag{20}
$$

where we have introduced $\underline{x}_{10} = \underline{w} - \underline{\zeta}$ and integrated over impact parameter, using the $k_T \cdot S_P$ term on the lhs to deduce the factor of $\underline{x}_{10} \times \underline{S}_P$ on the rhs in the last line.

In order to argue that this simplification is valid, it will be helpful to separately consider the quark exchange and gluon exchange terms within the polarized dipole amplitudes. For $G_{\underline{w}\underline{\zeta}}^i$ this is trivial, as the only subeikonal operator entering this dipole amplitude through the Wilson line $V_{\underline{x}}^i$ is a gluon exchange operator. For $G_{\underline{w}\underline{\zeta}}^{[2]}$, we can write

$$
G_{\underline{w}\underline{\zeta}}^{[2]} = G_{\underline{w}\underline{\zeta}}^{[2]g} + G_{\underline{w}\underline{\zeta}}^{[2]q}, \tag{21}
$$

with $G_{\underline{w}\underline{\zeta}}^{[2]g}$ containing the operators in the first line of Eq. (19b) and $G_{\underline{w}\underline{\zeta}}^{[2]q}$ containing those in the second line. For $G_{\underline{w}\underline{\zeta}}^{\text{mag}}$ we can make a similar decomposition as

$$
G_{\underline{w}\underline{\zeta}}^{\text{mag}} = G_{\underline{w}\underline{\zeta}}^{\text{mag}\,g} + G_{\underline{w}\underline{\zeta}}^{\text{mag}\,q}, \tag{22}
$$

with $G_{\underline{w}\underline{\zeta}}^{\text{mag}\,g}$ containing the operators in the first line of Eq. (13b), and $G_{\underline{w}\underline{\zeta}}^{\text{mag}\,q}$ containing those in the second line. Now we consider the gluon exchange component of the operator for the three polarized dipole amplitudes defined in Eq. (18). From [36,44] we know that, for a transversely polarized target, the gluon exchange dipole amplitudes $G_{\underline{w}\underline{\zeta}}^{[2]g}$

and $G_{\underline{w}\underline{\zeta}}^{\text{mag}\,g}$ have zero initial conditions. For $G_{\underline{w}\underline{\zeta}}^i$, we consider the correlator

$$
\left\langle \text{T tr}\left[V_{\underline{\zeta}} V_{\underline{w}}^{i\dagger}\right] - \text{T tr}\left[V_{\underline{w}}^i V_{\underline{\zeta}}^\dagger\right] \right\rangle. \tag{23}
$$

From [36,44] we know that for a transversely polarized target this correlator has a nonzero real term in its initial value. This real contribution comes from a triple gluon exchange between the dipole and the target, taking the gluons to be in the symmetric $d^{abc} = 2\text{tr}[\{t^a, t^b\}t^c]$ color representation, similar to how the Odderon (at leading order) comes from an eikonal triple gluon exchange in the color symmetric representation [3,81–84]. While the Odderon gives the imaginary part of the eikonal dipole amplitude (proportional to the eikonal Wilson line correlator $\langle\text{tr}[V_{\underline{x}} V_{\underline{y}}^\dagger]\rangle$), the similar initial condition for Eq. (23) is real due to an extra factor of i entering the subeikonal operator in Eq. (19a). In order to avoid a cancellation between a gluon exchange amplitude and the same amplitude with quark and antiquark interchanged as in Eq. (23), the correlator must be Odderon-like, and the extra i will make this a pure real contribution. Thus we find that $G_{\underline{w}\underline{\zeta}}^i$ has an initial condition of zero due to the "Im" operator in Eq. (18a).

As all of the initial conditions for polarized gluon exchange dipole amplitudes are zero, and we are studying the flavor nonsinglet worm-gear TMD, resumming polarized gluon emissions will not contribute to evolution because no flavor information would be communicated between the dipole and the target. One can consider a combination of polarized gluon and polarized quark emissions, but these terms would be suppressed by factors of N_c, so we will not include polarized gluon emissions in the linearized, large-N_c, DLA evolution equations which we consider here (cf. [17,23]). As we will see, the quark exchange dipole amplitudes do not contribute to $G_{\underline{w}\underline{\zeta}}^i$, $G_{\underline{w}\underline{\zeta}}^{[2]g}$ and $G_{\underline{w}\underline{\zeta}}^{\text{mag}g}$ through evolution, so these dipole amplitudes fully drop out of g_{1T}.

Now we turn to the quark exchange terms $G_{\underline{w}\underline{\zeta}}^{\text{mag}\,q}$ and $G_{\underline{w}\underline{\zeta}}^{[2]\,q}$. One can show that the Wilson line correlators in each of these polarized dipole amplitudes has pure real initial conditions (see Sec. III of [17] or Appendix B of [24]), so $G_{\underline{w}\underline{\zeta}}^{\text{mag}q}$ will have an initial condition of zero while $G_{\underline{w}\underline{\zeta}}^{[2]q}$ can be nonzero. We will find that these two dipole amplitudes do not mix under evolution, so $G_{\underline{w}\underline{\zeta}}^{\text{mag}q}$ drops out of the TMD and we are indeed left with only $G_{\underline{w}\underline{\zeta}}^{[2]q}$ entering in Eq. (20).

Having obtained the relevant polarized dipole amplitude for the small-x asymptotics of g_{1T}^{NS}, we now turn to its evolution. The only emissions which we need to consider for linearized, large-N_c, DLA evolution are unpolarized soft gluon (eikonal) emissions and polarized quark
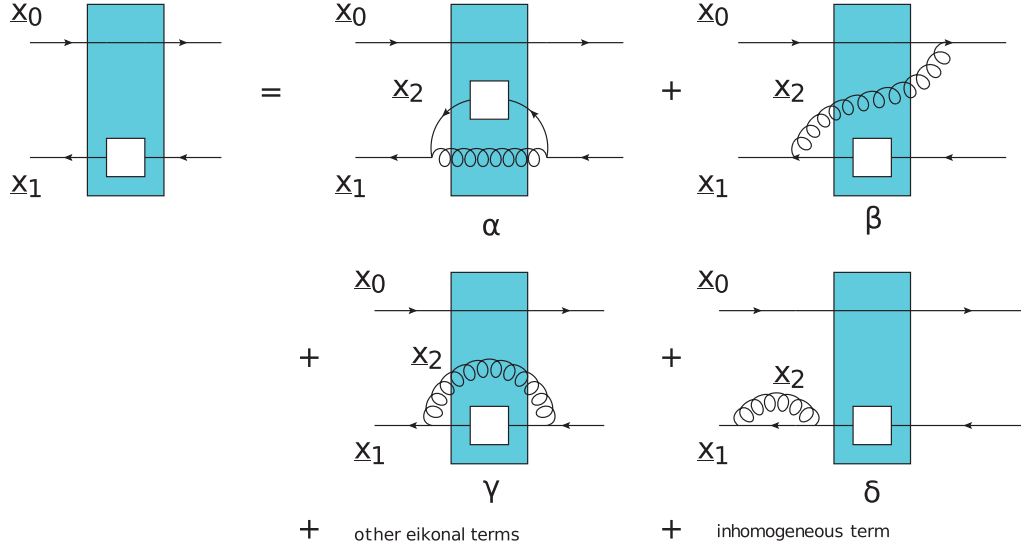
FIG. 2. The classes of diagrams contributing to the evolution of the amplitudes $G_{10}^{[2]}(z)$ from Eq. (18b). The diagram α on the right contains a sub-subeikonal soft-quark emission, while the remaining diagrams β, γ, δ, etc. are a sample of the eikonal emission diagrams [80,85–90].

emissions, as shown in Fig. 2. From [44] we know that the contributions from diagrams of class α vanish due to the tensor structure (the $\underline{x}_{10} \times \underline{S}_P$ factor) of the impact parameter integrated polarized dipole amplitude. Thus, we only have the eikonal, unpolarized soft gluon emissions to contend with. These emissions do not carry polarization information, and thus do not allow mixing between different polarized dipole amplitudes. We can see this diagrammatically by looking at the diagrams in classes β, γ, and δ in Fig. 2. In each diagram, the white box which symbolizes the polarization dependent subeikonal interaction is on the same antiquark line as it is in the diagram on the lhs of the figure, so the polarized Wilson line entering the dipole amplitude is the same on both sides.

Since there is no mixing of polarized dipole amplitudes through these emissions, a nonzero initial condition for $G_{w\underline{\zeta}}^{[2]}$ cannot generate a nonzero value for any of the other dipole amplitudes. Therefore, $G_{w\underline{\zeta}}^{[2]}$ is the only contributing dipole amplitude for the linearized small-x asymptotics. In the strict DLA, where one only allows for the polarization dependent quark exchange without any eikonal gluons exchanged in the initial condition of the polarized dipole amplitude, it can be shown that the real and virtual eikonal gluon emissions cancel for the leading-N_c initial conditions and evolution [17]. This would give a trivial evolution equation of the form

$$G_{w\underline{\zeta}}^{[2]}(zs) = G_{w\underline{\zeta}}^{[2](0)}(zs), \qquad (24)$$

with the dipole amplitude being given exactly by its initial condition $G_{w\underline{\zeta}}^{[2](0)}$. Such a cancellation of the class α

diagrams also occurred for the sub-subeikonal contribution to the Boer-Mulders function [44]. In that case the fact that the TMD was T-odd required a higher order initial condition, including an extra gluon exchange beyond the strict DLA. With this extra exchange, the sum over real and virtual eikonal gluon emissions is nonzero and allows for nontrivial small-x evolution. Here we can relax the DLA in the same way for the worm-gear TMD, summing over the eikonal gluon emissions to construct the evolution of the dipole amplitude $G_{w\underline{\zeta}}^{[2]}$. The resulting equation is identical to those obtained in Sec. III of [44], and yields the linearized, large-N_c asymptotics as

$$G^{[2]}(x_{10}^2, \zeta \ll 1) \sim \frac{1}{\zeta} J_1(2\zeta), \qquad (25)$$

where we have introduced the dimensionless variable $\zeta = \sqrt{\frac{\alpha_s N_c}{2\pi}} \ln(z \, s x_{10}^2)$. This is an oscillating solution with a decreasing amplitude, so the integral over z in the worm-gear TMD definition Eq. (20) will be dominated by the lower limit of the integral and the oscillations will have a negligible effect on the TMD. The resulting asymptotic scaling in x is

$$g_{1T}^{NS}(x \ll 1, k_T^2) \sim x^0. \qquad (26)$$

We find that the flavor nonsinglet worm-gear TMD g_{1T}^{NS} at small-x maintains its naive subeikonal scaling at DLA, having no dependence on the center of mass energy.

III. WORM-GEAR $h_{1L}^\perp$

Now we turn to the worm-gear $h_{1L}^\perp$, which can be interpreted as the number density of transversely polarized quarks within a longitudinally polarized proton. Its operator definition is [74]

$$
\frac{k_T^x}{M_P} h_{1L}^\perp(x, k_T^2) = \frac{1}{2} \sum_{S_P} S_P \int \frac{dr^- d^2 r_\perp}{2(2\pi)^3} \langle P, S_P | \bar{\psi}(0) \mathcal{U}[0, r]
$$

$$
\times \frac{i\sigma^{1+}\gamma_5}{2} \psi(r) | P, S_P \rangle
$$

$$
= \frac{1}{2} \sum_{S_P} S_P \int \frac{dr^- d^2 r_\perp}{2(2\pi)^3} \langle P, S_P | \bar{\psi}(0) \mathcal{U}[0, r]
$$

$$
\times \frac{\gamma_5 \gamma^+ \gamma^1}{2} \psi(r) | P, S_P \rangle, \tag{27}
$$

where the proton spin S_P is now in the longitudinal direction. We will again apply the LCOT, leading to an expression analogous to Eq. (9), but with $\gamma_5 \gamma^+ \gamma^1$ now projecting out the spinor structure. We need the anti BL spinor product

$$
\bar{v}_{\chi_2}(k_2) \frac{\gamma_5 \gamma^+ \gamma^1}{2} v_{\chi_1}(k_1)
$$

$$
= \frac{1}{2\sqrt{k_1^- k_2^-}} [im\delta_{\chi_1 \chi_2} \underline{S} \times (\underline{k}_1 - \underline{k}_2) - m\delta_{\chi_1, -\chi_2} \underline{S} \cdot (\underline{k}_1 + \underline{k}_2)
$$

$$
- \chi_1 \delta_{\chi_1 \chi_2} (2\underline{S} \cdot \underline{k}_1 \underline{S} \cdot \underline{k}_2 - \underline{k}_1 \cdot \underline{k}_2 - m^2)
$$

$$
- i\chi_1 \delta_{\chi_1, -\chi_2} (\underline{S} \times \underline{k}_1 \underline{S} \cdot \underline{k}_2 + \underline{S} \times \underline{k}_2 \underline{S} \cdot \underline{k}_1)], \tag{28}
$$

where $\underline{S} = \hat{x}$ is the direction of spin quantization for the quarks, and the spinors are now in the transverse spin basis which is related to the ordinary anti BL spinors by [3]

$$
u_\chi \equiv \frac{1}{\sqrt{2}} [u_+ + \chi u_-], \qquad v_\chi \equiv \frac{1}{\sqrt{2}} [v_+ + \chi v_-], \tag{29}
$$

where $\chi = \pm 1$. We also need the Wilson line replacement

$$
\bar{v}_{\chi_1}(k_1)(\hat{V}_{\underline{w}}^\dagger)^{ji} v_{\chi_2}(k_2) \to 2\sqrt{k_1^- k_2^-} (V_{\underline{w}; \chi_2 \chi_1}^{\text{pol}T\dagger})^{ji}, \tag{30}
$$

with

$$
V_{\underline{x}; \chi_2, \chi_1}^{\text{polT}} = \chi \delta_{\chi, \chi'} V_{\underline{x}}^{\text{T}} + \chi \delta_{\chi, -\chi'} V_{\underline{x}}^{\text{T}\perp}, \tag{31}
$$

containing polarized Wilson lines defined as

$$
V_{\underline{x}}^{\text{T}} \equiv \frac{g^2 (p_1^+)^2}{16 s^2} \int_{-\infty}^\infty dz_1^- \int_{z_1^-}^\infty dz_2^- V_{\underline{x}}[\infty, z_2^-] t^b \psi_\beta(z_2^-, \underline{x})
$$

$$
\times U_{\underline{x}}^{ba}[z_2^-, z_1^-] \Big[[i\gamma^5 \underline{S} \cdot \underline{\tilde{D}}_x - \underline{S} \times \underline{\tilde{D}}_x] \gamma^+ \gamma^-
$$

$$
+ [i\gamma^5 \underline{S} \cdot \underline{D}_x - \underline{S} \times \underline{D}_x] \gamma^- \gamma^+ \Big]_{\alpha\beta}
$$

$$
\times \bar{\psi}_\alpha(z_1^-, \underline{x}) t^a V_{\underline{x}}[z_1^-, -\infty], \tag{32a}
$$

$$
V_{\underline{x}}^{\text{T}\perp} \equiv -\frac{g^2 (p_1^+)^2}{16 s^2} \int_{-\infty}^\infty dz_1^- \int_{z_1^-}^\infty dz_2^- V_{\underline{x}}[\infty, z_2^-] t^b \psi_\beta
$$

$$
\times (z_2^-, \underline{x}) U_{\underline{x}}^{ba}[z_2^-, z_1^-] \Big[[i\underline{S} \cdot \underline{\tilde{D}}_x - \gamma^5 \underline{S} \times \underline{\tilde{D}}_x] \gamma^+ \gamma^-
$$

$$
+ [i\underline{S} \cdot \underline{D}_x - \gamma^5 \underline{S} \times \underline{D}_x] \gamma^- \gamma^+ \Big]_{\alpha\beta}
$$

$$
\times \bar{\psi}_\alpha(z_1^-, \underline{z}_1) t^a V_{\underline{x}}[z_1^-, -\infty]. \tag{32b}
$$

Taking the limit of massless quarks and performing the same simplifications as in Sec. III of [44] yields the leading, sub-subeikonal contribution to the worm-gear function as

$$
\frac{k_T^x}{M_P} h_{1L}^\perp(x, k_T^2) \subset \frac{2x(p_1^+)^2}{(2\pi)^3} \int d^2\zeta_\perp d^2 w_\perp \frac{d^2 k_{1\perp} dk_1^-}{(2\pi)^3} \frac{e^{i(\underline{k}_1 + \underline{k}) \cdot (\underline{w} - \underline{\zeta})} \theta(k_1^-)}{\underline{k}_1^2 \underline{k}^2} k_1^- \left(\frac{1}{\underline{k}_1^2} + \frac{1}{\underline{k}^2} \right) \Big[(\underline{S} \cdot \underline{k}_1 \underline{S} \cdot \underline{k} - \underline{k}_1 \cdot \underline{k})
$$

$$
\times \langle \text{Ttr}[V_{\underline{\zeta}} V_{\underline{w}}^{\text{T}\dagger}] + \bar{\text{T}} \, \text{tr}[V_{\underline{w}}^{\text{T}} V_{\underline{\zeta}}^\dagger] \rangle + i(\underline{S} \times \underline{k}_1 \underline{S} \cdot \underline{k} + \underline{S} \cdot \underline{k}_1 \underline{S} \times \underline{k}) \langle \text{Ttr}[V_{\underline{\zeta}} V_{\underline{w}}^{\text{T}\perp\dagger}] - \bar{\text{T}} \, \text{tr}[V_{\underline{w}}^{\text{T}\perp} V_{\underline{\zeta}}^\dagger] \rangle \Big]. \tag{33}
$$

We find the same polarized Wilson line correlators as in the case of the Boer-Mulders TMD, but with different tensor structures multiplying them. Subtracting the antiquark TMD contribution yields the flavor nonsinglet worm-gear TMD as

$$
\frac{k_T^x}{M_P} h_{1L}^{\perp \text{NS}}(x, k_T^2) = \frac{ixN_c}{\pi^3} \int d^2 x_{10} \frac{d^2 k_{1\perp}}{(2\pi)^3} e^{i(\underline{k}_1 + \underline{k}) \cdot \underline{x}_{10}} \frac{1}{\underline{k}_1^2 \underline{k}^2} \left(\frac{1}{\underline{k}_1^2} + \frac{1}{\underline{k}^2} \right) \int_{\frac{\Lambda^2}{s}}^1 \frac{dz}{z}
$$

$$
\times \left\{ (2\underline{S} \cdot \underline{k}_1 \underline{S} \cdot \underline{k} - \underline{k}_1 \cdot \underline{k}) H_{10}^1(z) + (\underline{S} \times \underline{k}_1 \underline{S} \cdot \underline{k} + \underline{S} \cdot \underline{k}_1 \underline{S} \times \underline{k}) H_{10}^2(z) \right\}, \tag{34}
$$

where we have the polarized dipole amplitudes

$$
H_{10}^1(z) \equiv \frac{1}{2N_c} \text{Im} \langle\langle \text{Ttr}[V_{\underline{0}} V_{\underline{1}}^{\text{T}\dagger}] - \text{Ttr}[V_{\underline{0}}^\dagger V_{\underline{1}}^{\text{T}}] \rangle\rangle_2, \tag{35a}
$$

$$
H_{10}^2(z) \equiv \frac{1}{2N_c} \text{Re} \langle\langle \text{Ttr}[V_{\underline{0}} V_{\underline{1}}^{\text{T}\perp\dagger}] - \text{Ttr}[V_{\underline{0}}^\dagger V_{\underline{1}}^{\text{T}\perp}] \rangle\rangle_2, \tag{35b}
$$

with the double angle brackets now scaling out two powers of energy and where again $\underline{x}_{10} = \underline{x}_1 - \underline{x}_0 = \underline{w} - \underline{\zeta}$. Noting that there is no ϵ^{ij} tensor structure on the lhs, we can see that the H^2_{10} term on the rhs needs to come in with an extra ϵ^{ij} after impact parameter integration, while the H^1_{10} term should only pick up a dot product term. We conclude that the impact parameter integrals of these two dipole amplitudes must have the structure

$$\int d^2 b_\perp H^1_{10}(z) = \underline{x}_{10} \times \underline{S} H^1(x^2_{10}, z), \qquad (36a)$$

$$\int d^2 b_\perp H^2_{10}(z) = \underline{x}_{10} \cdot \underline{S} H^2(x^2_{10}, z), \qquad (36b)$$

exactly as in the Boer-Mulders case [44].

The evolution of these dipole amplitudes is again given the diagrams in Fig. 2, and the same arguments as we applied above and as were applied for the Boer-Mulders TMD in [44] lead us to consider subleading N_c initial conditions which will be driven to small-x by eikonal gluon emissions. The resulting small-x asymptotics are

$$H^1(x^2_{10}, \zeta \ll 1) = H^2(x^2_{10}, \zeta \ll 1) \sim \frac{1}{\zeta} J_1(2\zeta), \qquad (37)$$

which gives the TMD scaling as

$$h^{\perp \text{NS}}_{1L}(x \ll 1, k^2_T) \sim \left(\frac{1}{x}\right)^{-1}. \qquad (38)$$

We find that, as with the Boer-Mulders TMD and the g_{1T} worm-gear TMD above, the flavor nonsinglet worm-gear $h^\perp_{1L}$ TMD at small-x maintains its naive sub-subeikonal scaling at DLA, falling off linearly with x.

IV. PRETZELOSITY $h^\perp_{1T}$

Finally we turn to the pretzelosity distribution, which has an operator definition as

$$\frac{k_T \cdot S_P k_T \times S_P}{M^2_P} h^{\perp q}_{1T}(x, k^2_T) = \epsilon^{ij} S^i_P \int \frac{dr^- d^2 r_\perp}{2(2\pi)^3} \langle P, S_P | \bar\psi(0)$$
$$\times \mathcal{U}[0, r] \frac{i\sigma^{j+}\gamma_5}{2} \psi(r) | P, S_P \rangle, \qquad (39)$$

where we can explicitly take the proton spin along the y-direction, $S_P = \hat{y}$, to simplify to

$$-\frac{k^x_T k^y_T}{M^2_P} h^{\perp q}_{1T}(x, k^2_T) = \int \frac{dr^- d^2 r_\perp}{2(2\pi)^3} \langle P, S_P | \bar\psi(0) \mathcal{U}[0, r]$$
$$\times \frac{\gamma_5 \gamma^+ \gamma^1}{2} \psi(r) | P, S_P \rangle. \qquad (40)$$

Once again the Dirac structure is projected out by $\gamma_5 \gamma^+ \gamma^1$, so we have the leading small-x contribution coming from the same sub-subeikonal structure as above in the worm-gear $h^\perp_{1L}$ [Eq. (33)]. Going straight to the flavor nonsinglet TMD, we have

$$-\frac{k^x_T k^y_T}{M^2_P} h^{\perp q\text{NS}}_{1T}(x, k^2_T)|_{\text{sub-subeik}} \subset \frac{ixN_c}{\pi^3} \int d^2 x_{10} \frac{d^2 k_{1\perp}}{(2\pi)^3} e^{i(\underline{k}_1 + \underline{k}) \cdot \underline{x}_{10}} \frac{1}{\underline{k}^2_1 \underline{k}^2} \left(\frac{1}{\underline{k}^2_1} + \frac{1}{\underline{k}^2}\right) \int^1_{\frac{\Lambda^2}{s}} \frac{dz}{z}$$
$$\times \left\{ (2\underline{S} \cdot \underline{k}_1 \underline{S} \cdot \underline{k} - \underline{k}_1 \cdot \underline{k}) H^{1T}(x_{10}, z) + (\underline{S} \times \underline{k}_1 \underline{S} \cdot \underline{k} + \underline{S} \cdot \underline{k}_1 \underline{S} \times \underline{k}) H^{2T}(x_{10}, z) \right\}. \qquad (41)$$

The dipole amplitudes entering here are defined again as

$$H^{1T}(x_{10}, z) \equiv \frac{1}{2N_c} \text{Im} \langle\langle \text{Ttr}[V_{\underline{0}} V^{T\dagger}_{\underline{1}}] - \text{Ttr}[V^\dagger_{\underline{0}} V^T_{\underline{1}}] \rangle\rangle_2, \quad (42a)$$

$$H^{2T}(x_{10}, z) \equiv \frac{1}{2N_c} \text{Re} \langle\langle \text{Ttr}[V_{\underline{0}} V^{T\perp\dagger}_{\underline{1}}] - \text{Ttr}[V^\dagger_{\underline{0}} V^{T\perp}_{\underline{1}}] \rangle\rangle_2, \quad (42b)$$

with double angle brackets again scaling out two powers of energy. The lhs of Eq. (41) is even under $k_T \to -k_T$, so integrating the dipole amplitudes over impact parameter cannot generate terms linear in $\underline{x}_{10}$ coupling to the spin vectors. This means that the diagrams in class α from Fig. 2 do not vanish. In the strict DLA limit the eikonal diagrams vanish, and we have the same contribution to evolution as for the polarized dipole amplitude contributing to the

transversity TMD in [23], with the class α diagrams yielding the linearized, large-N_c, DLA evolution for the dipole amplitudes as

$$H^{1T}_{10}(zs) = H^{1T(0)}_{10}(zs) + \frac{\alpha_s N_c}{2\pi} \int^z_{\Lambda^2/s} \frac{dz'}{z'} \int^{x^2_{10}z/z'}_{1/z's} \frac{dx^2_{21}}{x^2_{21}}$$
$$\times H^{1T}_{21}(z's), \qquad (43a)$$

$$H^{2T}_{10}(zs) = H^{2T(0)}_{10}(zs) + \frac{\alpha_s N_c}{2\pi} \int^z_{\Lambda^2/s} \frac{dz'}{z'} \int^{x^2_{10}z/z'}_{1/z's} \frac{dx^2_{21}}{x^2_{21}}$$
$$\times H^{2T}_{21}(z's), \qquad (43b)$$

where we have introduced the impact parameter integrated dipole amplitudes as

$$H_{10}^{1T}(zs) = \int d^2 b_\perp H^{1T}(x_{10}, zs), \qquad (44a)$$

$$H_{10}^{2T}(zs) = \int d^2 b_\perp H^{2T}(x_{10}, zs). \qquad (44b)$$

This equation can be solved analytically (cf. [23]), yielding the asymptotics for the flavor nonsinglet pretzelosity TMD as

$$h_{1T}^{\perp NS}(x \ll 1, k_T^2) \sim \left(\frac{1}{x}\right)^{-1 + 2\sqrt{\frac{\alpha_s N_c}{2\pi}}}, \qquad (45)$$

exactly matching the scaling of the corresponding transversity TMD.

V. CONCLUSIONS

In this paper we studied the small-x asymptotics of the flavor nonsinglet, leading-twist spin-spin coupling TMDs: the two worm-gear functions g_{1T} and $h_{1L}^\perp$, and the pretzelosity $h_{1T}^\perp$. We applied the LCOT, rewriting the operator definition of each TMD in the small-x limit in terms of polarized dipole amplitudes, and found that all three TMDs reduced essentially to polarized dipole amplitudes which are known from previous studies of other leading-twist TMDs. The close similarity of the contributing polarized dipole amplitudes means that the DLA, large-N_c, linearized small-x evolution for all three TMDs are known equations with known solutions, either through exact solutions or numerical calculations. We began with the flavor nonsinglet worm-gear TMD g_{1T}^{NS}, showing that it reduces to almost the same dipole amplitudes as the subeikonal contribution to the quark Sivers function [44], given in Eq. (18). The differences between the dipole amplitudes contributing to this worm-gear TMD and the Sivers function yield a substantial change by forcing most of the dipole amplitudes to have zero initial conditions, and the small-x asymptotics are controlled by polarized quark exchange operators. The tensor structure of the impact parameter integrated dipole amplitude makes the strict DLA small-x evolution trivial. Thus, we were led to consider the same eikonal gluon emission driven evolution as studied for the Boer-Mulders function [44], where going beyond the strict DLA limit was required by the T-odd nature of the TMD. This evolution yields an oscillating solution, where the oscillations of the dipole ultimately are washed out upon integrating over the internal momentum fraction variable z as in Eq. (20). Thus, the scaling of the TMD is unchanged from its naive subeikonal scaling, and we find

$$g_{1T}^{NS}(x \ll 1, k_T^2) = C_T(x, k_T^2)\left(\frac{1}{x}\right)^0 + \cdots, \qquad (46)$$

where the ellipses represent corrections which would come in at sub-subeikonal order.

Next we considered the flavor nonsinglet worm-gear TMD $h_{1L}^{\perp NS}$, which we found reduces to sub-subeikonal polarized dipole amplitudes Eq. (35) analogous to those which appear in the Boer-Mulders function. As with g_{1T}^{NS}, the tensor structure of the impact integrated dipole amplitudes [as shown in Eq. (36)] suggested that we consider the eikonal gluon emission driven evolution as studied for the Boer-Mulders function [44], yielding the same oscillating with decreasing amplitude behavior. Thus, the scaling of the TMD is unchanged from its naive sub-subeikonal scaling, and we find

$$h_{1L}^{\perp NS}(x \ll 1, k_T^2) = C_L(x, k_T^2)\left(\frac{1}{x}\right)^{-1} + \cdots \qquad (47)$$

It is important to note that there is a potential finite light quark mass correction proportional to m/k_T entering in at subeikonal order. The dipole amplitudes entering are again the same as in the case of the Boer-Mulders function, so the contributions would likely not evolve and yield an additive correction from the initial conditions. We leave a detailed investigation of the finite quark mass corrections for future work. The scaling of the evolved worm-gear TMDs g_{1T}^{NS} and $h_{1L}^{\perp NS}$ as x^0 and x respectively even after evolution is a very interesting feature. Based on the spin-dependent Odderon contribution to the eikonal quark Sivers function [11,21,36,44] and several gluon TMDs [7], which is known to maintain eikonal $(1/x)$ scaling under the effects of linear evolution [81,91–96], as well as the evolution of the sub-subeikonal Boer-Mulders TMD which maintains linear x scaling under linearized evolution, one might conjecture that there is some protection against evolution corrections coming from the T-odd property of all of these TMDs. With the two worm-gear functions we have examples of where the evolution effects again do not alter the naive sub-(sub)eikonal scaling as x for T-even TMDs, so if there is an underlying symmetry protecting these TMDs from evolution it is likely not determined by T-parity alone.

Finally, we studied the flavor nonsinglet pretzelosity TMD, where the small-x asymptotics came from polarized dipole amplitudes [Eq. (42)] analogous to the one entering the evolution of the quark transversity TMD. The evolution equations once again are already known, yielding the DLA, large-N_c, linearized asymptotics as

$$h_{1T}^{\perp NS}(x \ll 1, k_T^2) = C_{T\perp}(x, k_T^2)\left(\frac{1}{x}\right)^{-1 + 2\sqrt{\frac{\alpha_s N_c}{2\pi}}} + \cdots \qquad (48)$$

This is the same scaling as found in [23] for the flavor nonsinglet quark transversity TMD, which is a linear combination of h_{1T}^{NS} and $h_{1T}^{\perp NS}$, so indeed one would anticipate a match between the dipole amplitudes and

consequently the asymptotics. Again, there is a potential finite light quark mass correction to these results.

Combining the results in this study with those obtained for the quark helicity TMD [9,20,24,43,47], the quark transversity TMD [23], the quark Sivers and Boer-Mulders TMDs [7,11,21,36,44], as well as the asymptotics describing the unpolarized quark TMD [68,70], we have known small-x asymptotics for each of the leading twist quark TMDs, collected in Table I. Let us note a few interesting features of the table: first, the diagonal entries all have small-x scaling nearly equal to that of the Reggeon up to a factor of x. There appears to be some universality among the TMDs which survive k_T integration to yield the three flavor nonsinglet parton distribution functions (PDFs), although the pretzelosity TMD does not precisely fit in with this characterization. For the off diagonal entries, the leading terms are all exactly their naive scaling based on the quark spin content. The Sivers function is an unpolarized quark density and thus is eikonal, while the worm-gear g_{1T} is subeikonal due to probing the quarks' helicity, and the Boer-Mulders TMD and the worm-gear $h_{1L}^{\perp}$ are both sub-subeikonal due to probing the quarks' transversity. It may be that there is a symmetry protecting these off-diagonal TMDs from evolution effects based on the coupling between different directions of spin, as the quarks in these TMDs are all polarized in a different direction than their parent hadron (for example quark helicity with hadron transversity for g_{1T}).

Several of the leading-twist quark TMDs only have their small-x asymptotics calculated for the flavor nonsinglet functions, the flavor singlet functions which can mix with the gluon TMDs under evolution are a topic for future work. We note that the LCOT can be readily applied to gluon TMDs as in the case of the gluon helicity TMD [24,43], as the gluon TMDs are given by the adjoint representation versions of the polarized dipole amplitudes which enter into the flavor singlet quark TMDs. The flavor nonsinglet asymptotics which we have focused on here provide constraints on the valence quark distributions, giving crucial input for future TMD studies at the EIC [97–105]. These constraints can also be used in the global analysis of the available data for TMDs, as was done for the quark and gluon helicity using explicit small-x evolution in [106] and for the quark transversity using upper bounds from the small-x intercept in [107,108]. The use of explicit small-x evolution to constrain the global analysis in the small-x region and extrapolate beyond available data can in principle be applied to all eight leading-twist TMDs once the flavor singlet evolution equations have been obtained, allowing the current global analysis efforts [106–110] to extend further into the high energy regime of QCD. Having transversely and longitudinally polarized beams at the EIC will in principle allow for direct access to all of the TMDs listed in Table I in the small-x regime through various spin asymmetry measurements in SIDIS [69]. In order to fully probe the flavor nonsinglet TMDs multiple species of hadron beams will be required to achieve flavor separation.

We also note that the operator equations for the polarized dipole amplitudes have been constructed in the large-N_c limit, so one could go beyond the linearized DLA approximation used here to obtain precise phenomenological results. Going beyond the large-N_c limit, one could consider the large-N_c and N_f limit to restore quark contributions [24,31,43,106] where they have been neglected (for example in the subeikonal contribution to the Sivers function [44]). Obtaining evolution equations for all N_c values requires a generalization of the Jalilian-Marian-Iancu-McLerran-Weigert-Leodinov-Kovner (JIMWLK) equations [111–115] to include the subeikonal and sub-subeikonal operators needed for quark helicity dependent and quark transversity dependent insertions within the Wilson lines, as has been studied in [30,32].

ACKNOWLEDGMENTS

[1] F. Dominguez, C. Marquet, B.-W. Xiao, and F. Yuan, Phys. Rev. D **83**, 105005 (2011).

[2] F. Dominguez, J.-W. Qiu, B.-W. Xiao, and F. Yuan, Phys. Rev. D **85**, 045003 (2012).

[3] Y. V. Kovchegov and M. D. Sievert, Phys. Rev. D **86**, 034028 (2012).

[4] Y. V. Kovchegov and M. D. Sievert, Phys. Rev. D **89**, 054035 (2014).

[5] J. Zhou, Phys. Rev. D **89**, 074050 (2014).

[6] T. Altinoluk, N. Armesto, G. Beuf, M. Martinez, and C. A. Salgado, J. High Energy Phys. 07 (2014) 068.

[7] D. Boer, M. G. Echevarria, P. Mulders, and J. Zhou, Phys. Rev. Lett. **116**, 122001 (2016).

[8] Y. V. Kovchegov and M. D. Sievert, Nucl. Phys. **B903**, 164 (2016).

[9] Y. V. Kovchegov, D. Pitonyak, and M. D. Sievert, J. High Energy Phys. 01 (2016) 072.

[10] A. Dumitru, T. Lappi, and V. Skokov, Phys. Rev. Lett. **115**, 252301 (2015).

[11] L. Szymanowski and J. Zhou, Phys. Lett. B **760**, 249 (2016).

[12] Y. Hatta, Y. Nakagawa, F. Yuan, Y. Zhao, and B. Xiao, Phys. Rev. D **95**, 114032 (2017).

[13] Y. Hatta, B.-W. Xiao, S. Yoshida, and F. Yuan, Phys. Rev. D **94**, 054013 (2016).

[14] Y. Hatta, B.-W. Xiao, S. Yoshida, and F. Yuan, Phys. Rev. D **95**, 014008 (2017).

[15] D. Boer, Few-Body Syst. **58**, 32 (2017).

[16] I. Balitsky and A. Tarasov, J. High Energy Phys. 06 (2016) 164.

[17] Y. V. Kovchegov, D. Pitonyak, and M. D. Sievert, Phys. Rev. D **95**, 014033 (2017).

[18] Y. V. Kovchegov, D. Pitonyak, and M. D. Sievert, Phys. Rev. Lett. **118**, 052001 (2017).

[19] Y. V. Kovchegov, D. Pitonyak, and M. D. Sievert, Phys. Lett. B **772**, 136 (2017).

[20] Y. V. Kovchegov, D. Pitonyak, and M. D. Sievert, J. High Energy Phys. 10 (2017) 198.

[21] H. Dong, D.-X. Zheng, and J. Zhou, Phys. Lett. B **788**, 401 (2019).

[22] S. Benić and Y. Hatta, Phys. Rev. D **99**, 094012 (2019).

[23] Y. V. Kovchegov and M. D. Sievert, Phys. Rev. D **99**, 054033 (2019).

[24] Y. V. Kovchegov and M. D. Sievert, Phys. Rev. D **99**, 054032 (2019).

[25] G. A. Chirilli, J. High Energy Phys. 01 (2019) 118.

[26] T. Altinoluk and R. Boussarie, J. High Energy Phys. 10 (2019) 208.

[27] Y. V. Kovchegov, J. High Energy Phys. 03 (2019) 174.

[28] R. Boussarie, Y. Hatta, and F. Yuan, Phys. Lett. B **797**, 134817 (2019).

[29] R. Boussarie, Y. Hatta, L. Szymanowski, and S. Wallon, Phys. Rev. Lett. **124**, 172501 (2020).

[30] F. Cougoulic and Y. V. Kovchegov, Phys. Rev. D **100**, 114020 (2019).

[31] Y. V. Kovchegov and Y. Tawabutr, J. High Energy Phys. 08 (2020) 014.

[32] F. Cougoulic and Y. V. Kovchegov, Nucl. Phys. **A1004**, 122051 (2020).

[33] T. Altinoluk, G. Beuf, A. Czajka, and A. Tymowska, Phys. Rev. D **104**, 014019 (2021).

[34] Y. V. Kovchegov and M. G. Santiago, Phys. Rev. D **102**, 014022 (2020).

[35] A. Bacchetta, F. G. Celiberto, M. Radici, and P. Taels, Eur. Phys. J. C **80**, 733 (2020).

[36] Y. V. Kovchegov and M. G. Santiago, J. High Energy Phys. 11 (2021) 200.

[37] G. A. Chirilli, J. High Energy Phys. 06 (2021) 096.

[38] T. Altinoluk and G. Beuf, Phys. Rev. D **105**, 074026 (2022).

[39] D. Adamiak, Y. V. Kovchegov, W. Melnitchouk, D. Pitonyak, N. Sato, and M. D. Sievert (Jefferson Lab Angular Momentum Collaboration), Phys. Rev. D **104**, L031501 (2021).

[40] Y. V. Kovchegov, A. Tarasov, and Y. Tawabutr, J. High Energy Phys. 03 (2022) 184.

[41] S. Bondarenko, S. Pozdnyakov, and A. Prygarin, Eur. Phys. J. C **81**, 793 (2021).

[42] K. Banu, N. Vasim, and R. Abir, Phys. Rev. D **105**, 114033 (2022).

[43] F. Cougoulic, Y. V. Kovchegov, A. Tarasov, and Y. Tawabutr, J. High Energy Phys. 07 (2022) 095.

[44] Y. V. Kovchegov and M. G. Santiago, J. High Energy Phys. 11 (2022) 098.

[45] S. Benić, D. Horvatić, A. Kaushik, and E. A. Vivoda, Phys. Rev. D **106**, 114025 (2022).

[46] Y. Hatta and J. Zhou, Phys. Rev. Lett. **129**, 252002 (2022).

[47] J. Borden and Y. V. Kovchegov, Phys. Rev. D **108**, 014001 (2023).

[48] M. Li, J. High Energy Phys. 07 (2023) 158.

[49] L. V. Gribov, E. M. Levin, and M. G. Ryskin, Phys. Rep. **100**, 1 (1983).

[50] E. Iancu and R. Venugopalan, The color glass condensate and high-energy scattering in QCD, in *Quark-Gluon Plasma 4*, edited by R. C. Hwa and X.-N. Wang (2003), pp. 249–3363.

[51] H. Weigert, Prog. Part. Nucl. Phys. **55**, 461 (2005).

[52] J. Jalilian-Marian and Y. V. Kovchegov, Prog. Part. Nucl. Phys. **56**, 104 (2006).

[53] F. Gelis, E. Iancu, J. Jalilian-Marian, and R. Venugopalan, Annu. Rev. Nucl. Part. Sci. **60**, 463 (2010).

[54] J. L. Albacete and C. Marquet, Prog. Part. Nucl. Phys. **76**, 1 (2014).

[55] Y. V. Kovchegov and E. Levin, *Quantum Chromodynamics at High Energy* (Cambridge University Press, Cambridge, England, 2012), Vol. 33.

[56] A. Morreale and F. Salazar, Universe **7**, 312 (2021).

[57] S. Wallon, Acta Phys. Pol. B Proc. Suppl. **16**, 26 (2023).

[58] J. C. Collins and D. E. Soper, Nucl. Phys. **B194**, 445 (1982).

[59] J. C. Collins and D. E. Soper, Nucl. Phys. **B193**, 381 (1981).

[60] J. C. Collins and D. E. Soper, Nucl. Phys. **B197**, 446 (1982).

[61] J. C. Collins, D. E. Soper, and G. F. Sterman, Nucl. Phys. **B250**, 199 (1985).

[62] J. C. Collins, D. E. Soper, and G. F. Sterman, Adv. Ser. Dir. High Energy Phys. **5**, 1 (1988).

[63] R. Kirschner and L. Lipatov, Nucl. Phys. **B213**, 122 (1983).

[64] R. Kirschner, Z. Phys. C **31**, 135 (1986).

[65] R. Kirschner, Z. Phys. C **67**, 459 (1995).

[66] R. Kirschner, Z. Phys. C **65**, 505 (1995).

[67] S. Griffiths and D. Ross, Eur. Phys. J. C **12**, 277 (2000).

[68] K. Itakura, Y. V. Kovchegov, L. McLerran, and D. Teaney, Nucl. Phys. **A730**, 160 (2004).

[69] P. J. Mulders and R. D. Tangerman, Nucl. Phys. **B461**, 197 (1996); **B484**, 538(E) (1997).

[70] B. I. Ermolaev, S. I. Manaenkov, and M. G. Ryskin, Z. Phys. C **69**, 259 (1996).

[71] J. Bartels, B. Ermolaev, and M. Ryskin, Z. Phys. C **70**, 273 (1996).

[72] R. Kirschner, L. Mankiewicz, A. Schafer, and L. Szymanowski, Z. Phys. C **74**, 501 (1997).

[73] G. P. Lepage and S. J. Brodsky, Phys. Rev. D **22**, 2157 (1980).

[74] S. Meissner, A. Metz, and K. Goeke, Phys. Rev. D **76**, 034002 (2007).

[75] L. D. McLerran and R. Venugopalan, Phys. Rev. D **49**, 2233 (1994).

[76] L. D. McLerran and R. Venugopalan, Phys. Rev. D **49**, 3352 (1994).

[77] L. D. McLerran and R. Venugopalan, Phys. Rev. D **50**, 2225 (1994).

[78] Y. V. Kovchegov, Phys. Rev. D **54**, 5463 (1996).

[79] I. Balitsky, AIP Conf. Proc. **407**, 953 (1997).

[80] I. Balitsky, Phys. Rev. D **60**, 014020 (1999).

[81] Y. V. Kovchegov, L. Szymanowski, and S. Wallon, Phys. Lett. B **586**, 267 (2004), dedicated to the memory of Jan Kwiecinski, arXiv:hep-ph/0309281.

[82] Y. Hatta, E. Iancu, K. Itakura, and L. McLerran, Nucl. Phys. **A760**, 172 (2005).

[83] A. Kovner and M. Lublinsky, J. High Energy Phys. 02 (2007) 058.

[84] S. Jeon and R. Venugopalan, Phys. Rev. D **71**, 125003 (2005).

[85] A. H. Mueller, Nucl. Phys. **B415**, 373 (1994).

[86] A. H. Mueller and B. Patel, Nucl. Phys. **B425**, 471 (1994).

[87] A. H. Mueller, Nucl. Phys. **B437**, 107 (1995).

[88] I. Balitsky, Nucl. Phys. **B463**, 99 (1996).

[89] Y. V. Kovchegov, Phys. Rev. D **60**, 034008 (1999).

[90] Y. V. Kovchegov, Phys. Rev. D **61**, 074018 (2000).

[91] J. Bartels, L. Lipatov, and G. Vacca, Phys. Lett. B **477**, 178 (2000).

[92] Y. V. Kovchegov, AIP Conf. Proc. **1523**, 335 (2013).

[93] S. Caron-Huot, J. High Energy Phys. 05 (2015) 093.

[94] R. C. Brower, M. Djuric, and C.-I. Tan, J. High Energy Phys. 07 (2009) 063.

[95] E. Avsar, Y. Hatta, and T. Matsuo, J. High Energy Phys. 03 (2010) 037.

[96] R. C. Brower, M. S. Costa, M. Djurić, T. Raben, and C.-I. Tan, J. High Energy Phys. 02 (2015) 104.

[97] A. Accardi et al., Eur. Phys. J. A **52**, 268 (2016).

[98] D. Boer et al., arXiv:1108.1713.

[99] Proceedings, Probing Nucleons and Nuclei in High Energy Collisions: Dedicated to the Physics of the Electron Ion Collider: Seattle (WA), United States, 2018, edited by A. Prokudin, Y. Hatta, Y. Kovchegov, and C. Marquet (World Scientific Publishing, Singapore, 2020), arXiv:2002.12333.

[100] R. Abdul Khalek et al., Nucl. Phys. **A1026**, 122447 (2022).

[101] R. Abdul Khalek et al., arXiv:2203.13199.

[102] S. Amoroso et al., Acta Phys. Pol. B **53**, 12 (2022).

[103] R. Abir et al., arXiv:2305.14572.

[104] V. D. Burkert et al., Prog. Part. Nucl. Phys. **131**, 104032 (2023).

[105] M. Hentschinski et al., Acta Phys. Pol. B **54**, 3 (2023).

[106] D. Adamiak, Y. V. Kovchegov, and Y. Tawabutr, Phys. Rev. D **108**, 054005 (2023).

[107] C. Cocuzza, A. Metz, D. Pitonyak, A. Prokudin, N. Sato, and R. Seidl, arXiv:2308.14857.

[108] C. Cocuzza, A. Metz, D. Pitonyak, A. Prokudin, N. Sato, and R. Seidl (JAM Collaboration), arXiv:2306.12998.

[109] S. Bhattacharya, Z.-B. Kang, A. Metz, G. Penn, and D. Pitonyak, Phys. Rev. D **105**, 034007 (2022).

[110] M. Bury, A. Prokudin, and A. Vladimirov, J. High Energy Phys. 05 (2021) 151.

[111] J. Jalilian-Marian, A. Kovner, A. Leonidov, and H. Weigert, Nucl. Phys. **B504**, 415 (1997).

[112] J. Jalilian-Marian, A. Kovner, A. Leonidov, and H. Weigert, Phys. Rev. D **59**, 014014 (1998).

[113] J. Jalilian-Marian, A. Kovner, and H. Weigert, Phys. Rev. D **59**, 014015 (1998).

[114] E. Iancu, A. Leonidov, and L. D. McLerran, Phys. Lett. B **510**, 133 (2001).

[115] E. Iancu, A. Leonidov, and L. D. McLerran, Nucl. Phys. **A692**, 583 (2001).